

## Tongue muscle fiber tracking during rest and tongue protrusion with oral appliances: A preliminary study with diffusion tensor imaging

Hideo Shinagawa<sup>1,\*</sup>, Emi Z. Murano<sup>1</sup>, Jiachen Zhuo<sup>2</sup>, Bennett Landman<sup>3</sup>,  
Rao P. Gullapalli<sup>2</sup>, Jerry L. Prince<sup>3</sup> and Maureen Stone<sup>1</sup>

<sup>1</sup>Department of Biomedical Sciences, University of Maryland Baltimore,  
650 W Baltimore St., Baltimore, MD 21201 U.S.A.

<sup>2</sup>Department of Diagnostic Radiology, University of Maryland Baltimore,  
22 S. Greene St., Baltimore, MD 21201 U.S.A.

<sup>3</sup>Department of Biomedical Engineering, The Johns Hopkins University of Medicine,  
Baltimore, MD 21205 U.S.A.

(Received 28 September 2007, Accepted for publication 8 January 2008)

**Keywords:** Human tongue, *In vivo*, Deformation, DTI, Fiber tracking, Oral appliance  
**PACS number:** 43.70.Aj [doi:10.1250/ast.29.291]

### 1. Introduction

Diffusion tensor imaging (DTI) is an emerging method for imaging tissue. It is an enhancement of the basic principals of magnetic resonance imaging (MRI) and has been in use since 1990 for imaging structures of white matter in the central nervous system [1,2], and since 1995 for imaging peripheral myoarchitecture such as the heart [3], the calf [4] and the tongue [5] in the *in vivo* human.

The tongue has a very complex myoarchitecture consisting of extrinsic and intrinsic muscles, which control the various oral functions of mastication, swallowing, and articulation. Extrinsic muscles (e.g., genioglossus (GG), hyoglossus, styloglossus (SG) and palatoglossus) have bony origins; their fibers course in many directions within the tongue before inserting into the tongue. Intrinsic muscles (superior longitudinalis, verticalis, transverses, and inferior longitudinalis (IL)), on the other hand, originate, course, and insert within the tongue. The IL and SG muscles are addressed in this paper because it plays an important role in controlling precise tongue tip and body retraction [6].

DTI uses changes in the MRI signal caused by the Brownian motion, or *diffusion*, of water molecules within a tissue. Cell membranes restrict water diffusion thereby yielding an orientation dependent (i.e., anisotropic) signal property, which is modeled by a three-dimensional (3D) tensor. Tractography [7–9] is component postprocessing technique that tracks fiber orientation given a 3D array of diffusion tensors. It enables non-invasive 3D depiction of fiber structure orientation. The principal eigenvector is assumed to correspond to the predominant fiber orientation and connected fiber regions are discovered by following the orientation of one voxel to the next and tracking connected voxels throughout the image volume. Each fiber trajectory can be rendered in 3D and colored to indicate its local orientation (see Fig. 1).

Methods such as electropalatography (EPG) [10], X-ray cineradiography [11], ultrasound [12], and cine-MRI [13] have been used to visualize tongue surface movements during

oral functions [14,15]. Additionally, both histology and anatomy [16,17] have clarified the interdigitation of the tongue muscles *ex vivo*. However, the orientation and deformation of tongue muscle bundles are not well defined *in vivo*. The purpose of this study was to depict tongue muscle fiber deformation *in vivo*, especially IL and SG muscle fibers during both rest and tongue protrusion with oral appliances.

### 2. Material and methods

Two healthy adult volunteers (1 female and 1 male) with no history of oral diseases or other medical conditions participated in the study. Informed consent, which explained all the experiment procedures, was obtained from each subject. This study had approval from the Humans Research Protections Office of the University of Maryland, School of Medicine, Baltimore, U.S.A.

Measurements were performed with a 1.5T MR machine (Magnetom Avanto, Siemens, Erlangen, Germany). A head and neck coil was used to obtain the DTI data. Axial slices (23 slices for subject 1 and 28 slices for subject 2) were localized to parallel the mandibular surface and to cover the whole tongue of each subject.

The DTI data were acquired using a spin-echo echo planar imaging (EPI) technique with diffusion weighting applied along 6 directions, a b-value of 500 s/mm<sup>2</sup>, and 4 averages [5,18]. Using a b-value much lower than is customary in DTI imaging of white matter was critical to achieving high quality DTI in the tongue. Other imaging parameters included a field of view (FOV) of 200 × 200 mm, a slice thickness of 3 mm, TR of 5,000 ms, TE of 66 ms, voxel size of 3.1 × 3.1 × 3.0 mm, and matrix size of 64 × 64. Diffusion gradients were applied with a twice-refocused spin echo scheme to reduce eddy currents. GRAPPA parallel imaging was used with an acceleration factor of 2. DTI images were taken during both rest and tongue protrusion and each acquisition time was about 3 minutes.

Additionally, high resolution spin-echo T2 weighted axial images as reference images were also taken for both conditions (i.e., rest and tongue protrusion) with the following

\*e-mail: HShinagawa@umaryland.edu

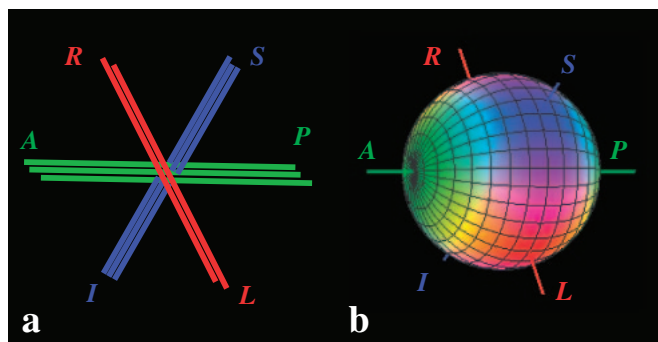


**Fig. 1** Each color indicates local fiber direction (a) in 3D coordinate space as indicated by the colored sphere (b). Green, blue and red indicate anterior-posterior (A-P), superior-inferior (S-L), right-left (R-L) fiber orientation, respectively.

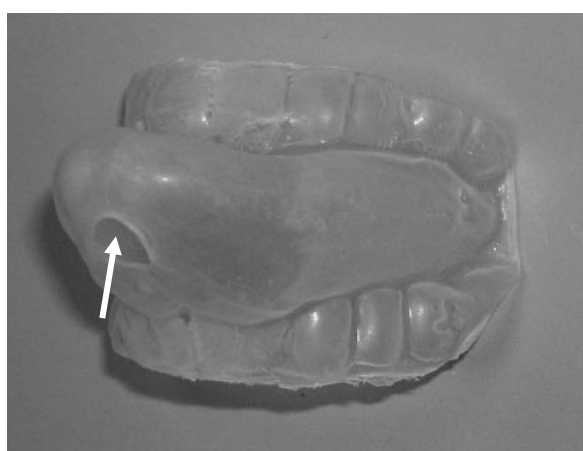


**Fig. 2** The oral appliance is modified by drilling a hole on the inferior surface at the anterior tongue (white arrow). A vacuum hose is connected to the hole, thereby immobilizing the tongue and extracting saliva during MRI acquisitions.

parameters: FOV = 160 × 160 mm, slice thickness = 3 mm, TR = 3,000 ms, TE = 99 ms, voxel size = 0.8 × 0.6 × 3.0 mm, and matrix size = 256 × 256. The axial slices were localized to match in the numbers (i.e., 23 slices for subject 1 and 28 slices for subject 2), thickness (i.e., 3 mm), and position (i.e., parallel to the mandibular surface) to the DT slices.

During tongue protrusion, each subject had a custom-fabricated oral appliance (Fig. 2), which is often used for obstructive sleep apnea patients. Before the experiments, the subjects had silicone impressions to transfer the tongue protrusion shape accurately to the plaster cast. The oral appliances were made of a flexible polyvinyl material (Raintree ESSIX, Metairie, LA), using the plaster cast. In this study, each appliance was further modified by drilling a hole with a diameter of about 10 mm (see Fig. 2) for suctioning saliva, and creating a vacuum to fixate the tongue. The appliance also fixed the jaws during the MRI acquisitions because it was attached to the upper and lower teeth by dental adhesive before the scanning, which further reduced motion.



**Fig. 3** High resolution T2 sagittal images at rest (A) and tongue protrusion with an oral appliance (B) in subject 1. The white arrow indicates the location of the vacuum hose.

The DTI data analysis and tractography were performed using dTV-II implemented in VOLUME-ONE software, which was provided by the VOLUME-ONE development group (University of Tokyo, <http://ut-radiology.umin.jp>). The threshold for the tractography was set at fractional anisotropy (FA) > 0.18 [2,5].

### 3. Results

Figure 3 shows the high resolution T2 mid-sagittal images during rest (A) and tongue protrusion (B) in subject 1. The tongue shape differences between the two conditions were confirmed clearly, as were differences in locations of muscle masses. Especially, the tip and surface of the tongue during tongue protrusion were different from those at rest. The tip was pulled forward and there was clearance between the palate and surface of the tongue during tongue protrusion with oral appliances.

Tongue muscle fiber interdigitation at rest is shown in Fig. 4. Figure 4B is a high resolution T2 coronal image of the head with the tongue circled (yellow). To extract muscle fibers in DTI, a region of bundled fibers must be known. The high resolution T2 image was used to manually identify regions of interest (ROIs) including GG, MH, and IL plus SG bundled fibers (see Fig. 4A). Figures 4C and E show coronal and oblique views, respectively, of the fibers that were independently tracked from these manually identified regions. The IL and SG muscle fibers are shown in green course horizontally (anterior-posterior) at both sides of the tongue (Figs. 4C and E). GG is shown in blue (vertical) and green (horizontal), because it has a fan-shaped fiber orientation. Mylohyoid (MH) is shown in red, purple, and blue at the bottom of the tongue. MH muscle fibers course laterally at the bottom of the tongue like the arc of a circle (Fig. 4E).

Comparisons were made between rest and tongue protrusion for IL and SG, as shown in axial slices in Fig. 5. Red lines represent the mandible. At rest (A), the IL and SG muscle fibers exhibited its characteristic anterior-posterior fiber orientation, and also a V-shape configuration which is narrower anteriorly. IL and SG was more stretched anteriorly, increased in length, and had a more constant width during protrusion (Fig. 5B).

### 4. Discussion

It is difficult to maintain still tongue protrusion during MRI acquisitions. Motion artifacts due to swallowing and

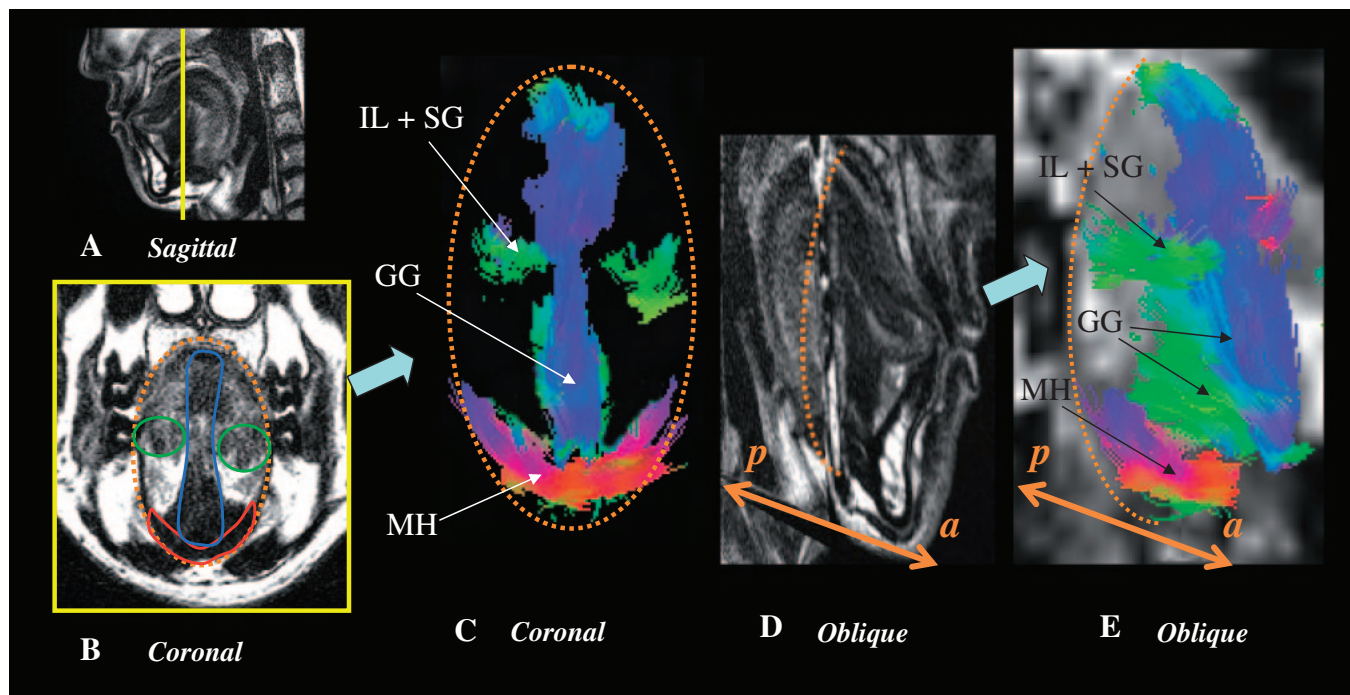


**Fig. 4** The yellow line in the high resolution T2 mid-sagittal image (A) indicates the location of the coronal views (B and C). In addition, to show the same location of the tongue, the orange circles and semicircles are used in coronal (B and C) and oblique views (D and E), respectively. Three regions of interest (ROIs) represent genioglossus (blue), inferior longitudinalis and styloglossus (green), and mylohyoid (red). Tractography is shown in coronal (C) and oblique (E) views. Abbreviation: GG; genioglossus, IL; inferior longitudinalis, SG; styloglossus, MH; mylohyoid, *a*; anterior, *p*; posterior. The colors in the tractography denote the fiber directions (see Fig. 1). In oblique view (E), the fan-shaped fiber orientation of GG is indicated by the change in color (i.e., blue to green).

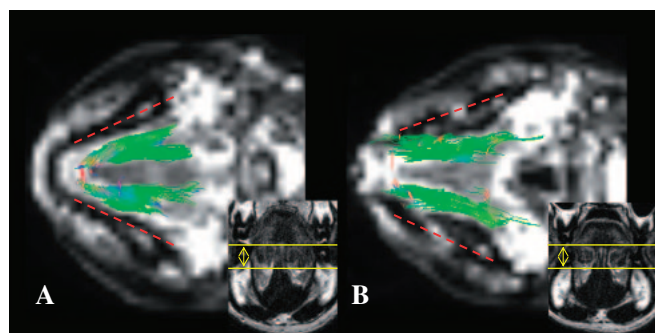


**Fig. 5** Axial slices at rest (A) and tongue protrusion (B). During tongue protrusion with an oral appliance, the inferior longitudinalis (IL) and styloglossus (SG) muscles are longer, thinner, and more parallel. The red dashed lines are the mandibular bones and serve as landmarks to compare muscle fiber orientation between the two conditions. The selected slice thickness for the muscle fiber tracking is 15 mm in each condition and the locations are shown in the coronal images below.

small motion during tongue protrusion were reduced by using the oral appliance with a hole for suctioning saliva and creating a vacuum to fixate the tongue (Fig. 2). This was a technical advantage for this study. The interdigitation of the tongue muscle fibers in the *in vivo* human was depicted well with DTI tractography, and the result was consistent with

previous studies [5,16,17]. Identification of GG, MH, and IL was facilitated by their anatomy: they have bundled regions and they are located at the center or bottom of the tongue, which minimizes the geometric artifact caused by saliva and air.

In the study, we could not segregate IL and SG muscle fibers completely because they are adjacent. However, the deformation of IL and SG muscle fibers was depicted distinctly between rest and tongue protrusion with oral appliances. Protrusion caused stretch in IL and SG: it was thinner, longer, more parallel, and more anterior. This finding suggests that DTI has the potential to extract fiber orientation not only for muscle structure, but also for muscle deformation in the *in vivo* human tongue.

In conclusion, tongue muscle fibers were depicted *in vivo* during both rest and tongue protrusion with oral appliances. It might be possible to visualize tongue muscle fiber deformation during oral functions such as speech. Further studies for the deformation in the *in vivo* human tongue are needed for tracking the fiber orientation more clearly and precisely.

**Acknowledgement**

Some of this material was presented at the 4th joint meeting of ASA/ASJ in Hawaii. The research was supported by Japan Society for the Promotion of Science (JSPS)-Postdoctoral Fellowships for Research Abroad and National Institute on Deafness and Other Communication Disorders (NIDCD) grant R01-01758.

## References

- [1] M. E. Moseley, Y. Cohen, J. Kucharczyk, J. Mintorovitch, H. S. Asgari, M. F. Wendland, J. Tsuruda and D. Norman, "Diffusion-weighted MR imaging of anisotropic water diffusion in cat central nervous system," *Radiology*, **176**, 439–445 (1990).
- [2] P. J. Basser, J. Mattiello and D. LeBihan, "MR diffusion tensor spectroscopy and imaging," *Biophys. J.*, **66**, 259–267 (1994).
- [3] T. G. Reese, R. M. Weisskoff, R. N. Smith, B. R. Rosen, R. E. Dinsmore and V. J. Wedeen, "Imaging myocardial fiber architecture *in vivo* with magnetic resonance," *Magn. Reson. Med.*, **34**, 786–791 (1995).
- [4] S. Sinha, U. Sinha and V. R. Edgerton, "*In vivo* diffusion tensor imaging of the human calf muscle," *J. Magn. Reson. Imaging*, **24**, 182–190 (2006).
- [5] T. A. Gaige, T. Benner, R. Wang, V. J. Wedeen and R. J. Gilbert, "Three dimensional myoarchitecture of the human tongue determined *in vivo* by diffusion tensor imaging with tractography," *J. Magn. Reson. Imaging*, **26**, 654–661 (2007).
- [6] M. Stone and A. Lundberg, "Three-dimensional tongue surface shapes of English consonants and vowels," *J. Acoust. Soc. Am.*, **99**, 3728–3737 (1996).
- [7] R. Bammer, B. Acar and M. E. Moseley, "*In vivo* MR tractography using diffusion imaging," *Eur. J. Radiol.*, **45**, 223–234 (2003).
- [8] S. Mori and P. C. van Zijl, "Fiber tracking: principles and strategies—A technical review," *NMR Biomed.*, **15**, 468–480 (2002).
- [9] S. Wakana, A. Caprihan, M. M. Panzenboeck, J. H. Fallon, M. Perry, R. L. Gollub, K. Hua, J. Zhang, H. Jiang, P. Dubey, A. Blitz, P. van Zijl and S. Mori, "Reproducibility of quantitative tractography methods applied to cerebral white matter," *Neuroimage*, **36**, 630–644 (2007).
- [10] H. Y. Cheng, B. E. Murdoch, J. V. Goozee and D. Scott, "Electropalatographic assessment of tongue-to-palate contact patterns and variability in children, adolescents, and adults," *J. Speech Lang. Hear. Res.*, **50**, 375–392 (2007).
- [11] J. R. Green and Y. T. Wang, "Tongue-surface movement patterns during speech and swallowing," *J. Acoust. Soc. Am.*, **113**, 2820–2833 (2003).
- [12] V. Parthasarathy, M. Stone and J. L. Prince, "Spatiotemporal visualization of the tongue surface using ultrasound and Kriging (SURFACES)," *Clin. Linguist. Phonet.*, **19**, 529–544 (2005).
- [13] M. Stone, E. P. Davis, A. S. Douglas, M. N. Aiver, R. Gullapalli, W. S. Levine and A. J. Lundberg, "Modeling tongue surface contours from Cine-MRI images," *J. Speech Lang. Hear. Res.*, **44**, 1026–1040 (2001).
- [14] K. M. Hiimae, J. B. Palmer, S. W. Medicis, J. Hegener, B. S. Jackson and D. E. Lieberman, "Hyoid and tongue surface movements in speaking and eating," *Arch. Oral Biol.*, **47**, 11–27 (2002).
- [15] V. Sanguineti, R. Laboissière and Y. Payan, "A control model of human tongue movements in speech," *Biol. Cybern.*, **77**, 11–22 (1997).
- [16] A. Iskander and I. Sanders, "Morphological comparison between neonatal and adult human tongues," *Ann. Otol. Rhinol. Laryngol.*, **112**, 768–776 (2003).
- [17] H. Takemoto, "Morphological analyses of the human tongue musculature for three-dimensional modeling," *J. Speech Lang. Hear. Res.*, **44**, 95–107 (2001).
- [18] C. Pierpaoli, P. Jezzard, P. J. Basser, A. Barnett and G. Di Chiò, "Diffusion tensor MR imaging of the human brain," *Radiology*, **201**, 637–648 (1996).